EUROPEAN ORGANIZATION FOR NUCLEAR RESEARCH

CERN AT/94-05 (DI)
CERN SL/94-04 (AP)
LHC Note 264

Luminosity Considerations for Different Ion Species

D. Brandt, K. Eggert, and A. Morsch

Abstract

The maximal achievable luminosity for heavy ion collisions is principally limited by the short lifetimes which are a consequence of the large beam-beam cross-sections. The two main processes, the electromagnetic dissociation of the ions and the creation of an electron-positron pair with subsequent electron capture, have strong Z-dependencies. This could lead to much higher luminosities for ions lighter than Pb. We calculate the luminosity lifetime and the average luminosity for a realistic running scenario taking into account the beam-beam effects and the intra beam scattering. Only based on lifetime arguments the luminosity for Nb-Nb (Ca-Ca) collisions could be three (four) orders of magnitude larger than for Pb-Pb collisions. This assumes that appropriate sources and accumulation schemes could be found. These large luminosities for ions with medium masses are relevant for rare quark-gluon plasma signals, like muon-pair production, and for two photon physics.

Geneva, Switzerland
3 March 1994

1. Introduction

Heavy ion physics belongs to the heart of the Large Hadron Collider (LHC) programme. For Pb-Pb collisions the maximum luminosities are seven orders of magnitude below the proton collisions. This is due to the large cross-sections (order of 300 barn) of electromagnetic processes which either disintegrate the ions or change their charge due to electron capture. Since these processes have a strong dependence on the ion charge Z, much larger luminosities are expected for lighter ions. In this paper we calculate the maximal possible luminosities for different ion species which can be obtained if a sufficient number of ions can be stored in the LHC.

The main goal of the heavy ion physics, the proof and analysis of a quark-gluon plasma, can be tackled either with the analysis of particle compositions and correlations in minimum bias events or with the study of the production of heavy vector mesons, like the J/ψ or the Y families. For the former case luminosities of about 10^{27} $cm^{-2}s^{-1}$ are already saturating the data taking on these central events. The vector mesons in the latter process are identified via their decays into lepton pairs and occur with a rate of about 10^{-3} s^{-1} (for J/ψ) per central event. To be able to accumulate the necessary large statistics, lepton triggers are mandatory and luminosities around 10^{30} $cm^{-2}s^{-1}$ are beneficial. The signal for a quark-gluon plasma is the J/ψ suppression which can also be faked by absorption in a hadron gas scenario. However, the dependence on the energy density is different for the two scenarios; e.g. there is a complete suppression in both scenarios at energy densities in Pb collisions (> 8 GeV/fm^3) whereas in Ca collisions (4 GeV/fm^3) one expects a complete suppression in the quark-gluon plasma scenario and a factor 5 for absorption in a hadron gas (see answers of the ALICE collaboration to the LHCC). Furthermore, the background conditions change with the ion species since the particle multiplicity is proportional to $A^{4/3}$. To cope with the lower production cross-sections for lighter ions (A^2-dependence) increased luminosities are needed.

Colliding heavy ions are effectively an intense source of quasi-real photons and hence allow the study of two-photon coherent collisions. The cross-section is proportional to Z^4. A luminosity of 4 10^{30} $cm^{-2}s^{-1}$ for Ca collisions is therefore equivalent to 6 10^{35} $cm^{-2}s^{-1}$ for e^+e^- colliders. The physics case has been stressed in an ALICE note by S. Sadovski (ALICE/93-07). The events, with the two colliding ions intact, exhibit low particle multiplicity which facilitates the detection of new particles compared to the central ion collisions with their huge multiplicities. Heavy quarkonium states with even C- parity, such as η_c, η_b or η_t can be directly produced which is not the case in e^+e^- collisions. The cross-sections fall with $1/m_{\gamma\gamma}^3$ which explains the need for large luminosities for high mass particle searches. The coupling strength to quarks is proportional to the fourth power of the quark charge which makes the two photon process an analyser of the quark content of the produced particles. Photon collisions may also be the best place to search for states with four quarks or for hybrid states with gluons involved. At very high luminosities one may even dream of production of charged boson pairs, Higgses or of exotic particles beyond the Standard Model. Whereas the study of two photon physics is interesting in itself it also provides a laboratory for new particle production, if luminosities are sufficiently large.In summary, runs with different ion species and enhanced luminosities enlarge considerably the potential for heavy ion physics.

2. Luminosity Lifetime

The luminosity L at LHC is given by the number of bunches k and the luminosity per bunch L_{bunch} which depends on the number of particles per bunch N and the transverse beam radius σ_t, both varying with time [1,2]:

$$L = kL_{bunch} \propto \frac{N^2}{\sigma_t^{\,2}} \tag{1}$$

The number of particles per bunch is decreased by the interaction of the particles in the crossing points (beam-beam) and the interactions with the rest gas in the vacuum chamber (beam-gas)[2]. In the case of heavy ions in the LHC, the cross-sections for beam-beam interactions are huge, exceeding 300 barn for Pb-Pb collisions. The rest gas in the vacuum chamber, however, is very much reduced with respect to the proton case since it originates from the synchrotron radiation which is at least a factor 30 smaller in the ion case. The lower currents for very heavy ions, like Pb, further reduce the synchrotron radiation and more than compensates for an increase in the beam-gas cross-sections. The rest gas density without synchrotron radiation is at least a factor 100 lower compared to the nominal proton case [3]. Hence beam-gas interactions can be neglected in the luminosity lifetime calculations.

The beam decay time t_{bb} is inversely proportional to the initial number of ions per bunch N_0, the number of interaction points n_x and the total cross-section σ_{tot} but is independent of the number of bunches k:

$$N(t) = \frac{N_0}{1+\frac{t}{t_{bb}}} \quad \text{with} \quad t_{bb} = \frac{N_0}{\sigma_{tot} L^0_{bunch} n_x} \propto \frac{1}{\sigma_{tot} N_0 n_x} \tag{2}$$

The luminosity half lifetime $t_{1/2}$ is related to the beam lifetime through:

$$t_{1/2} = \left(\sqrt{2}-1\right) t_{bb} \tag{3}$$

The strong increase of the total ion cross-section with the atomic number of the ion is limiting the maximal achievable luminosity.

An additional effect is the intra-beam scattering (IBS) which blows-up the beam dimensions during the run [4]. The scattering cross-section is proportional to the square of the classical ion radius, i.e. $\sim Z^4/A^2$, where Z denotes the charge and A the mass number of the ion. Remembering that all the parameters entering the IBS calculations (longitudinal and transverse emittances, energy factor) have their own A and Z dependencies, in the high energy limit, the IBS beam growth rate scales in good approximation like NZA [1].

The emittance blow-up after a sufficiently small time step Δt can be approximated as:

$$\varepsilon_{x,z,l}(t+\Delta t)=\left(1+\frac{\Delta t}{\tau_{x,z,l}(\sigma,\ N,\ldots)}\right)\varepsilon_{x,z,l}(t) \tag{4}$$

Here, $\varepsilon_{x,z,l}$ are the transverse (x,z) and longitudinal (l) emittances and $1/\tau_{x,z,l}$ are the respective emittance growth rates characterising the process. They are themselves functions of the beam dimensions and the number of particles per bunch.

To calculate the time evolution of the luminosity, one has to find a self consistent solution of the particle loss equation including the beam radius growth $\sigma_t(t,N)$:

$$\frac{1}{N}\frac{\mathrm{d}N}{\mathrm{d}t}=-\frac{1}{t_{\mathrm{bb}}}\frac{N}{N_0}=-const.\ \frac{N(t)}{\sigma_t^{\,2}(t,N(t))} \tag{5}$$

Since for any realistic scenario $N(t)$ is a well behaved, monotonically falling function its solution can be found by simple numerical integration. The function is sampled in sufficiently small time intervals Δt. At each sampling point one calculates the intra-beam scattering growth rates and the luminosity which determine, respectively, the beam blow-up and the particle loss in the next time step.

2.1 Beam-Beam Interactions

Mainly three processes contribute to beam-beam interactions where the ions are lost from the beam:

(1) Hadronic nuclear interactions [5].

(2) Electromagnetic dissociation where an ion is excited by a γ–nucleon interaction and subsequently decays [6,7,8]. The largest contribution to this process comes from the excitation of the giant dipole resonance which decays mainly by particle emission or fission.

(3) Two photon process creating an electron positron pair and the subsequent capture (mainly K-shell) of the electron by an ion [6,9].

The nature of the collision process, electromagnetic or nuclear, depends upon the value of the impact parameter.

The hadronic nuclear interaction is dominant when the colliding ions overlap. Hence, the nuclear interaction rate increases approximately with the geometrical overlap of the two ions. A reasonable description of present data provides the hard-sphere overlap parametrization of Bradt and Peters [10].

$$\sigma_{nuc}=\sigma_0\left(\mathrm{A}_1^{\,1/3}+\mathrm{A}_2^{\,1/3}-b\right)^2, \tag{6}$$

where A_1, A_2 are the mass numbers of the two ions and $\sigma_0 \sim 70$ mb and b~1.3. A more refined description is the semi classical optical model of P. J. Karol [11] which also provides analytical expressions for the nuclear cross-section.

The electromagnetic processes, in contrast, involve impact parameters much larger than the range of nuclear forces. Their relative importance rapidly increases with the charge Z of the ions. The electromagnetic interaction of the peripheral colliding ions can be described by the reaction of equivalent photons (Weizsäcker-Williams method of virtual quanta [7]). Thereby a photon can either directly react with one of the nuclei or two photons are scattered.

In Pb-Pb collisions at LHC, photons are produced over a wide energy range, even up to ~500 TeV. Considering photon-nucleus scattering, the photon energy range comprises the region of the giant dipole resonance (E_γ~0.006-0.04 GeV), quasi deuteron and Δ resonances (0.04-2 GeV) and non-resonant scattering (>2 GeV). A calculation of the total electromagnetic dissociation cross-section making use of the available experimental results for γ Pb scattering up to 80 GeV can be found in Ref. [8]. The result for LHC (Pb-Pb) is 222 barn which includes an estimated cross section of 16 barn for the energy range above 80 GeV guided by the latest HERA results. Note that this number (222 barn) is larger than that used so far in the LHC calculation (180 barn).

The $\gamma\gamma$ reaction can produce lepton pairs. Relevant in our context is the production of e^+-e^- pairs which, for Pb-Pb collisions at LHC, has the huge cross-section of 2.6 10^5 barn. However, only if one of the ions captures the electron it will be lost, since its charge is reduced by one. Because the capture probability is low the resulting e^--capture cross-section amounts only to 101 barn [9] but it gives still a sizeable contribution to the total cross-section.

Simple A and Z dependencies for the individual cross-sections have been derived for the individual processes [6]. We use these relations in order to calculate the cross sections for ions lighter than Pb. Normalising to the Pb-Pb results of Refs. [8,9] one obtains:

- Electromagnetic Dissociation at the Giant Dipole Resonance

$$\sigma_{\mathrm{GDR}} \approx 67.5 \frac{(A-Z)Z^3}{A^{2/3}} \quad (\mu\mathrm{b}), \tag{7a}$$

- Electromagnetic Dissociation above the Giant Dipole Resonance

$$\sigma_{ED} \approx 108 A^{0.9} Z^2 \quad (\mu\mathrm{b}), \tag{7b}$$

- e^--capture

$$\sigma_{e^-e^-} \approx 2.1\ 10^{-6} \frac{Z^8}{e^{2\pi\alpha Z} - 1} \quad (\mu\mathrm{b}), \tag{7c}$$

In Fig. 1, the total cross-sections and the cross-sections for the individual processes are plotted as a function of the ion charge using *A* and *Z* of the most common stable nuclei. The nuclear cross sections calculated with the semi classical optical model of Ref. [11] using nuclear radii from Ref. [12] are shown as points for some selected ion pairs (p-p, He-He, O-O, Ca-Ca, Nb-Nb, and Pb-Pb). Above Z~20 the electromagnetic dissociation process has the largest cross-section and a significant contribution from e^--capture is expected for Z>40. Below Z=20 the nuclear cross-section is dominant. The individual ion-ion cross sections for the ion species considered in this report are shown in Table 1.

Table 1: *Cross sections for ion-ion interactions (in barn).*

	Nuclear	e.m. Dissoc.	e^--Capture	Total
Pb_{82}^{208}	7.8	222	101	336
Nb_{41}^{97}	4.9	23.4	3.1	31.4
Ca_{20}^{40}	3.1	2.1	$4\ 10^{-2}$	5.2
0_8^{16}	1.5	0.12	$8\ 10^{-5}$	1.6
He_2^4	0.35	$2\ 10^{-3}$	$6\ 10^{-9}$	0.35
p	0.105	-	$5\ 10^{-11}$	0.105

2.2 Intra Beam Scattering (IBS)

IBS is the multiple Coulomb scattering of particles within a bunch, which causes a diffusion process and an exchange of energy between synchrotron and betatron oscillations. The theory of IBS was developed by A. Piwinski (1974) [4]. In the limit of high energies one obtains for the longitudinal and transverse emittances growth rates the following approximate formulae [13,14]:

$$\frac{1}{\tau_l} = \frac{1}{\varepsilon_l}\frac{d\varepsilon_l}{dt} = C\left(1-d^2\right) \tag{8a}$$

$$\frac{1}{\tau_x} = \frac{1}{\varepsilon_x}\frac{d\varepsilon_x}{dt} = 2Cd^2 \tag{8b}$$

$$\frac{1}{\tau_z} = \frac{1}{\varepsilon_z}\frac{d\varepsilon_z}{dt} \approx 0 \tag{8c}$$

The emittances are connected to the *rms* beam-sizes $\sigma_{x,z}$ at the interaction point (no dispersion) and the relative *rms* energy spread σ_E through:

$$\varepsilon_{x,z} = \frac{\sigma_{x,z}{}^2}{\beta^*_{x,z}}\gamma \tag{9a}$$

$$\varepsilon_l = 4\pi\sigma_E E\frac{\sigma_l}{c}, \tag{9b}$$

where β^* denotes the value of the β-function at the interaction point, σ_l the bunch length, E the particle energy and c the velocity of light. The beam growth is driven by the increase of the longitudinal energy spread produced by the scattering process. Through the dispersion of the machine the growth of the energy spread is coupled to the transverse direction (x) parallel to the bending of the dipoles. The dimensionless coupling parameter d is given by:

$$d = \frac{\sigma_E}{\hat{\sigma}_x}\hat{D} \ , \tag{10}$$

Here, $\hat{\sigma}_x$ denotes the *rms* horizontal beam size and $\hat{D}$ the dispersion of the machine, both values averaged over the ring circumference. The common parameter C of equations (8a,b) is proportional to the square of the classical ion radius r_0, the phase space density $N/\varepsilon_x\varepsilon_z\varepsilon_l$, the ion rest mass E_0 and to a complicated scattering integral (F) which is usually solved numerically. For a fixed machine design the growth rates scale like NAZ:

$$C = \frac{1}{16\pi} r_0^{\,2} \frac{N}{\varepsilon_x \varepsilon_z \varepsilon_l} E_0 \frac{F}{\gamma} \propto NAZ, \tag{11}$$

The original theory of IBS considered an ideal machine without coupling between the transverse planes nor vertical dispersion. In such a model, the vertical beam size is predicted to slowly shrink as a function of time. Experimentally, due to the above mentioned effects, one observes that the beams stay round. The luminosity is inversely proportional to the geometrical mean of the horizontal and vertical emittances, i.e. $\sim 1/\sqrt{(\varepsilon_x\varepsilon_z)}$. Thus for the calculation of the luminosity lifetime it is irrelevant, whether one dimension blows up and the other slowly shrinks or the beam stays round and both dimensions blow up but with half of the rate calculated with (8b).

Inserting the standard LHC parameters [15] for Pb-Pb collisions listed in Table 2, C amounts to 2.2 10^{-5} s^{-1} and d amounts to 0.7. For arbitrary A, Z and N one obtains for the initial transverse emittance growth time:

$$\tau_{x,z} = 26\text{h}\ \frac{208}{A}\ \frac{82}{Z}\ \frac{9.4\ 10^7}{N} \tag{12}$$

The parameters determining the growth time change with the collider running time through particle losses and the intra-beam scattering process itself. This leads to a relative fast blow-up at the beginning and a slower growth at the end of the run.

2.3 Average Luminosity

The number of signal events accumulated during a given collider running time is given by the integrated luminosity (average luminosity times running time) . A realistic calculation of the average luminosity for a running cycle of the LHC must take into account the filling time 't_f' of the machine and the waiting time 't_w' when the beams are colliding but experiments are still down [16]. Thus, the average luminosity for a collider operating in physics conditions for a time 't_r' is:

$$\frac{\langle L\rangle}{L_0} = \frac{1}{t_f + t_r}\int_{t_w}^{t_r} \frac{L(t)}{L_0}\,dt \qquad (13)$$

For the following calculations we used t_f = 4h and t_w =1/3 h as standard parameters.

Table 2: ***Standard LHC Parameters for the Heavy Ion*** **(Pb-Pb)** ***Mode*** **[15].**

Atomic Number of Pb	Z	82
Mass Number of Pb	A	208
Initial Luminosity	L_0	$1.6\ 10^{27}$ cm^{-2} s^{-1}
Initial Number of Ions/Bunch	N_0	$9.4\ 10^7$
Number of Bunches	k	496
Bunch Occupation	k/k_0	0.752
Revolution Frequency	f	11.2 kHz
Initial Beam Current	I_0	84 µA •Z
Bunch Interval	Δt	134.7 ns
Ion Energy	E	7 TeV •Z
γ	E/m_p	7516 •Z/A
β-value at Interaction Point	β^*	0.5 m
Transverse Normalised Emittance	ε_n	3.75 µm •Z/A
Longitudinal Emittance	$\varepsilon_l = 4\pi\,\sigma_s/c\sigma_E E$	5 eVs •Z
Relative *rms* Energy Spread	σ_E	$1.3\ 10^{-4}$
Crossing Angle	ϕ	<100 µrad
Average β	$\hat{\beta}$	62 m
Average Dispersion	$\hat{D}$	1.29 m
Luminosity half lifetime	$t_{1/2}$	7.8 h

3. Results for Different Ion Species

The parameters for heavy ion collisions used in the following calculations are derived from the standard LHC parameters for Pb-Pb collisions listed in Table 2 [15]. As mentioned above, some of the parameters change with Z or Z/A as indicated in this Table.

Figs. 2a-c show the time evolution of the normalised luminosity (L/L_0) and the average luminosity ($\langle L\rangle/L_0$) for the ions Pb (A=208, Z=82), Ca (A=40, Z=20) and He (A=4, Z=2). The number of ions per bunch was tuned such that the luminosity half-lifetime amounts to 10 h for one experiment, which corresponds to $\langle L\rangle/L_0 = 0.45\ L_0$ after 20h running time. In order to get a feeling for the relative importance of beam-beam interactions and IBS we plot as a solid line the time evolution when all processes are included and as a dashed line the corresponding result without IBS. In the case of Pb, the luminosity decrease is totally dominated by the beam-beam interaction. For ions with Z in the range of 10 to 40 (like Ca) IBS has its maximum influence and for the light ions (below Z=10) the latter effect is again very small.

As shown previously, the luminosity lifetime due to beam-beam losses and IBS strongly decreases with increasing atomic number and is inversely proportional to the number of ions per bunch. Thus, fixing the luminosity lifetime to 10 h, the number of ions per bunch can be increased going from a heavy to a lighter ion. Since the luminosity is proportional to the square of the number of ions per bunch, a significant increase in luminosity can be expected. In order to get a comprehensive understanding of the effects of going to lighter ion species, we show in Figs. 3a,b the luminosity half lifetime for different ion species (Pb, Nb, Ca, O, He and p) as a function of the initial number of ions per bunch and the corresponding initial luminosity per bunch. In Fig. 3a we assumed 1 experiment and 2 experiments in Fig. 3b. The horizontal displacements of the curves measure the increases in luminosity for a fixed luminosity lifetime.

The important 'figure of merit' for the collider performance is the average luminosity after a certain running time. In Fig. 4, we show the average luminosity after 20h of running for the different ion species as a function of the initial number of ions per bunch and the corresponding initial luminosities.

Assuming a lifetime of 10h and 1 experiment, the initial luminosity can be increased by a factor 70 going from Pb to Nb and by a factor 2000 going down to Ca ions. For 2 experiments at equal luminosities, we see that the increases in luminosity are factors 90 and 2500, respectively. Furthermore, doubling the number of experiments decreases the luminosity by a factor 3.3 at Pb but only by a factor 2.7 at Nb, reflecting the reduced importance of the beam-beam interaction for lighter ion species.

Table 3: *Initial luminosities (upper values in units of* $cm^{-2}s^{-1}$) *and number of ions per beam (lower values) at fixed luminosity lifetime* ($t_{1/2}$ = 10 h).

	1Exp./25 ns	**1Exp./135 ns**	**2Exp./25 ns**	**2Exp./135 ns**	**3Exp./25 ns**	**3Exp./135 ns**
p	$6.9\ 10^{34}$	$1.2\ 10^{34}$	$1.9\ 10^{34}$	$3.3\ 10^{33}$	$8.7\ 10^{33}$	$1.5\ 10^{33}$
	$7.5\ 10^{14}$	$1.3\ 10^{14}$	$3.9\ 10^{14}$	$6.8\ 10^{13}$	$2.8\ 10^{14}$	$4.6\ 10^{13}$
He_2^4	$5.7\ 10^{33}$	$9.9\ 10^{32}$	$1.7\ 10^{33}$	$2.9\ 10^{32}$	$7.8\ 10^{32}$	$1.4\ 10^{32}$
	$2.1\ 10^{14}$	$3.7\ 10^{13}$	$1.2\ 10^{14}$	$2.0\ 10^{13}$	$7.9\ 10^{13}$	$1.4\ 10^{13}$
0_8^{16}	$1.7\ 10^{32}$	$2.9\ 10^{31}$	$5.7\ 10^{31}$	$9.9\ 10^{30}$	$2.9\ 10^{31}$	$5.0\ 10^{30}$
	$3.7\ 10^{13}$	$6.3\ 10^{12}$	$2.1\ 10^{13}$	$3.7\ 10^{12}$	$1.5\ 10^{13}$	$2.6\ 10^{12}$
Ca_{20}^{40}	$1.0\ 10^{31}$	$1.8\ 10^{30}$	$4.0\ 10^{30}$	$6.9\ 10^{29}$	$2.3\ 10^{30}$	$3.9\ 10^{29}$
	$9.2\ 10^{12}$	$1.6\ 10^{12}$	$5.7\ 10^{12}$	$1.0\ 10^{12}$	$4.3\ 10^{12}$	$7.4\ 10^{11}$
Nb_{41}^{97}	$3.7\ 10^{29}$	$6.4\ 10^{28}$	$1.4\ 10^{29}$	$2.4\ 10^{28}$	$7.4\ 10^{28}$	$1.3\ 10^{28}$
	1.710^{12}	$3.0\ 10^{11}$	$1.0\ 10^{12}$	$1.8\ 10^{11}$	$7.7\ 10^{11}$	$1.3\ 10^{11}$
Pb_{82}^{207}	$5.2\ 10^{27}$	$8.9\ 10^{26}$	$1.6\ 10^{27}$	$2.7\ 10^{26}$	$8.0\ 10^{26}$	$1.4\ 10^{26}$
	$2.0\ 10^{11}$	$3.5\ 10^{10}$	$1.1\ 10^{11}$	$2.0\ 10^{10}$	$8.0\ 10^{10}$	$1.4\ 10^{10}$

Table 3 gives an overview of the initial luminosity and total number of ions per beam at fixed luminosity lifetime ($t_{1/2}$ = 10 h) for all ion species considered in this report. In addition to the values for the nominal Pb-Pb bunch spacing of 135 ns (k=496), we quote the corresponding numbers for a 25 ns bunch spacing scenario (k=2870 [1]).

4. Two-Photon Physics with Different Ion Species

The large luminosities for ions with light and medium masses cause large photon fluxes such that two-photon physics might be attractive. As an example, we consider the lepton pair production. Its cross-section is proportional to the fourth power of the ion charge and inversely proportional to the lepton mass m_l squared and depends only weakly on the Lorentz factor γ:

$$\sigma_{\ell^+\ell^-} = \frac{224}{27\pi}\alpha^2\frac{(Ze)^4}{m_\ell^2}\ln^3\gamma \tag{15}$$

Inserting the LHC Pb-Pb parameters one obtains for the muon-pair production cross section $\sigma_{\mu^+\mu^-}$=6.1 barn. This cross-section can be scaled to other ion species:

$$\sigma_{\ell^+\ell^-}^{LHC} = 6.1\left(\frac{Z}{82}\right)^4\left(\frac{106\text{MeV}}{m_\ell}\right)^2\times\left(1.12+\frac{\ln\left(\frac{Z}{A}\right)}{8}\right)^3 \quad \text{(barn)} \tag{16}$$

Fig. 5 gives the muon pair yield for the luminosities of Table 3 (2 experiments and 25 ns bunch spacing) integrated over a collider running time of 20 hours. No efficiency cuts have been applied. The largest rates are for ions with a charge around 20 where with a rate of 50 kHz we expect events only containing one muon pair and nothing else. This may offer the hope that also larger invariant masses may be seen via the two-photon process.

On the other hand, at the highest luminosities of around 10^{34} $cm^{-2}s^{-1}$ about 1 kHz of muon pair events are expected for the proton case. It will be difficult to disentangle these low momentum (typically 0.5 - 1 GeV) muons in the bulk of the overlapping events. But at a luminosity of 10^{32} $cm^{-2}s^{-1}$, overlapping events are rare and almost empty events with only two muons can be easily triggered on and identified. It is interesting to note that these electromagnetic processes can be precisely calculated with an uncertainty of probably less than a percent [17] and hence may serve as an excellent luminosity calibration [18].

5. Injection Scheme for Lighter Ions

As discussed in the previous section, with respect to the luminosity lifetime much higher intensities could be envisaged for lighter ions as compared to Pb ions. However, it remains to be demonstrated that such intensities can be accommodated along the whole chain of injectors.

Keeping in mind that in the standard injection scheme retained for the Pb ions (including accumulation in LEAR) [19], the space charge effect already approaches its limits, it becomes obvious that the problem would be even worse for increased intensities of light ions. It thus follows that such a scheme cannot be envisaged. Both, the space charge problems and the accumulation of ions lighter than Pb is studied in detail in Ref. [20]. This report also presents a new scheme which consists in injecting the ions in LEAR with a low charge state and accelerating these ions to an energy high enough where they could be fully stripped just after extraction. In order to avoid expensive modifications of the machine, LEAR would work in a single bunch mode and the required accumulation would then take place in the PS. As clearly mentioned in Ref. [20], this new scheme still requires further investigations. However, it looks extremely promising, in the sense that it might satisfy the requirements imposed by high intensities of light ions in the LHC.

6. Conclusions

To operate the LHC with different ion species from He up to Pb is of general interest. Most of the heavy ion physics requires only low luminosity. However, high luminosities are required for the study of both lepton-pair production in hadronic collisions and two-photon processes with large invariant masses. Furthermore, it is interesting to point out that hadronic cross-sections for rare processes with large momentum transfer increase with A^2 and hence could also be studied in the collisions of light ions, provided sufficient luminosity could be obtained.

The maximum integrated luminosity is basically determined by the luminosity lifetime which is limited by the large cross-sections in the case of heavy ions. Their strong decrease with the ion-charge Z reduces the electromagnetic dissociation and the two-photon process below the hadronic cross-section for ions lighter than Ca. Consequently, the maximum luminosity for Ca (O) could be about three (four) orders of magnitude larger than for Pb, if appropriate accumulation schemes can be found.

Two-photon processes are of interest since they lead to lepton-pair production and at much lower rate to e.g. W^+W^- production. The largest rates are not obtained with Pb collisions but for ions with a charge around 20. The loss due to the Z^4-dependence of the cross-section is more than compensated by the potential gain with higher luminosities.

It is not only interesting to study new physics with the two photon process, but also to use the well known QED production of low-mass muon pairs for the measurement of the luminosity. This process can probably be calculated with a precision of the order of one percent. For proton collisions, the muon pair production via the two photon process has an expected rate of 10 Hz at a luminosity of 10^{32} cm^{-2}s^{-1} where the probability for overlapping events is small. The events have a clean signature with only two low momentum muons and the two intact protons.

At low luminosities the search for the quark-gluon plasma in minimum bias events is best done with central Pb collisions leading to the highest energy density. However, to extract signals for a quark-gluon plasma in the muon pair channel, like J/Ψ suppression, needs large statistics. Besides Pb, ions like Nb and Ca, are best suited since much larger luminosities should in principle be possible. It was stressed by the heavy-ion community that varying the ion species is essential for the study of the background and the extraction of a possible signal for a quark-gluon plasma.

We have shown the main luminosity limitations due to lifetime considerations. Whether the large ion currents can be really achieved in the LHC depends mainly on the source and the accumulation scheme and has to be studied in detail. If a sufficient number of ions could be accumulated, a bunch spacing of 25 ns would yield an additional factor of 5.8 in the luminosity compared to the proposed bunch structure of 135 ns. An additional advantage would then be that the bunch spacings for p-p and heavy-ion collisions would be the same which would lead to an easier running of the proton experiments on heavy ion collisions and vice versa.

References

[1] D. Brandt, *'Relativistic Heavy Ions in the LHC'*, SPS/AMS/Note/89-6, LHC/Note 87, (1989) and references therein.
D. Brandt, E. Brouzet, J. Gareyte, *'Heavy Ions in the SPS-LHC Complex'*, LHC Note 208.

[2] K. Hübner and E. Keil, IEEE Trans. Nucl. Sci., **32** (1985), 1632
E. Fischer, *'Residual Gas Scattering, Beam Intensity and Interaction Rate in Proton Storage Rings'*, CERN-ISR/67-16 (VA).

[3] A.G. Mathewson, Private Communication.

[4] A. Piwinski, Proc. 9th. Int. Conf. on High Energy Accelerators, SLAC, (1974)
A. Piwinski, *'Intra Beam Scattering'*, Proc. of the CERN Accelerator School, Noordwijkerhout (1991), CERN 92-01, pp 226-242.

[5] J. Bartke, J. Mod. Phys. **A4** (1989), 1319.

[6] G. Baur and C. A. Bertulani, Nucl. Phys. **A505** (1989), 835. and references therein.

[7] J. D. Jackson, Classical Electrodynamics, 2nd ed. (Wiley, New York), Chap. 15, p-619;
D. Olson et al., Phys. Rev. **C24** 1529 (1981).

[8] M. Vidovic, M. Greiner, and G. Soff, Phys. Rev. **C48** (1993), 2011.

[9] G. Baur and C. A. Bertulani, Phys. Rep. 163 (1988), 299.

[10] H.L. Bradt, B. Peters, Phys. Rev. **77** (1950), 54.

[11] P. J. Karol, Phys. Rev. **C11** (1975), 1203.

[12] G. Fey, Z. Phys. **256** (1973), 401.

[13] L. Evans, B. Zotter, CERN-SPS/80-15.

[14] L. Vos, *'Approximate Formulae for Intra Beam Scattering Calculations, Application to Protons in the SPS and the LHC, and Heavy Ions in the LHC'*, CERN-SPS/87-3 (AMS), LHC Note 64.

[15] The LHC Study Group, *'LHC: The Large Hadron Collider Accelerator Project'*, CERN-AC/93-03 (LHC).

[16] K. Eggert and A. Morsch, *'Luminosity Considerations for the LHC'*, CERN-AT/94-xx (DI).

[17] G. Baur, private communication.

[18] K. Eggert and A. Morsch, LHC Note in preparation.

[19] P. Levevre and D. Möhl, *'Lead Ion Accumulation Scheme for LHC'*, CERN-PS/93-45 (DI) and LHC Note 257.

[20] P. Levevre and D. Möhl, *'A Low Energy Accumulation Ring of Ions for LHC'*, CERN-PS/93-62 (DI) and LHC Note 259.

Figure Captions

Fig.1

Z-dependence of ion-ion partial cross-sections: total cross-section (solid line), electromagnetic dissociation (dashed line), pair production+electron capture (dotted line) and nuclear interactions for p-p, He-He, O-O, Ca-Ca, Nb-Nb and Pb-Pb collisions (solid points).

Fig. 2

Luminosity and average luminosity as a function of the collider running time for **(a)** Pb-Pb **(b)** Ca-Ca and **(c)** He-He collisions.

Fig 3

The luminosity half lifetime as a function of the of the initial number of ions per bunch (initial luminosity) for **(a)** 1 experiment and **(b)** 2 experiments.

Fig. 4

The average luminosity after 20 h of running as a function of the initial number of ions per bunch (initial luminosity) for **(a)** 1 experiment and **(b)** 2 experiments.

Fig. 5

Average muon pair production rate $\langle R \rangle_{\mu^+\mu^-}$ from the $\gamma\gamma$-process as a function of the atomic number Z. A bunch spacing of 25 ns and 2 experiments have been assumed.

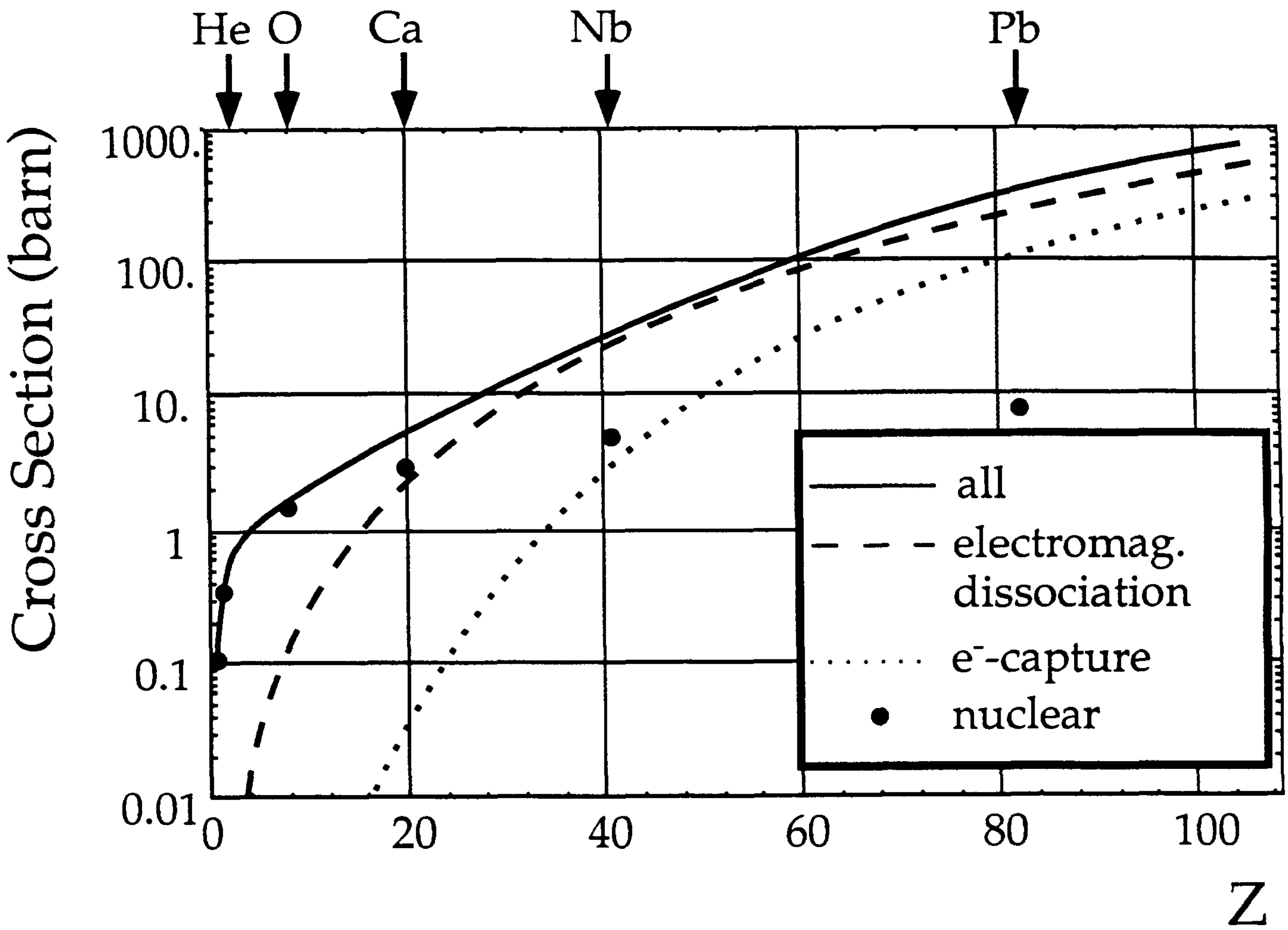
He
O
Ca
Nb
Pb
Cross Section (barn)
1000.
100.
10.
1
0.1
0.01
0
20
40
60
80
100
Z
all
electromag. dissociation
e⁻-capture
nuclear

Fig. 1

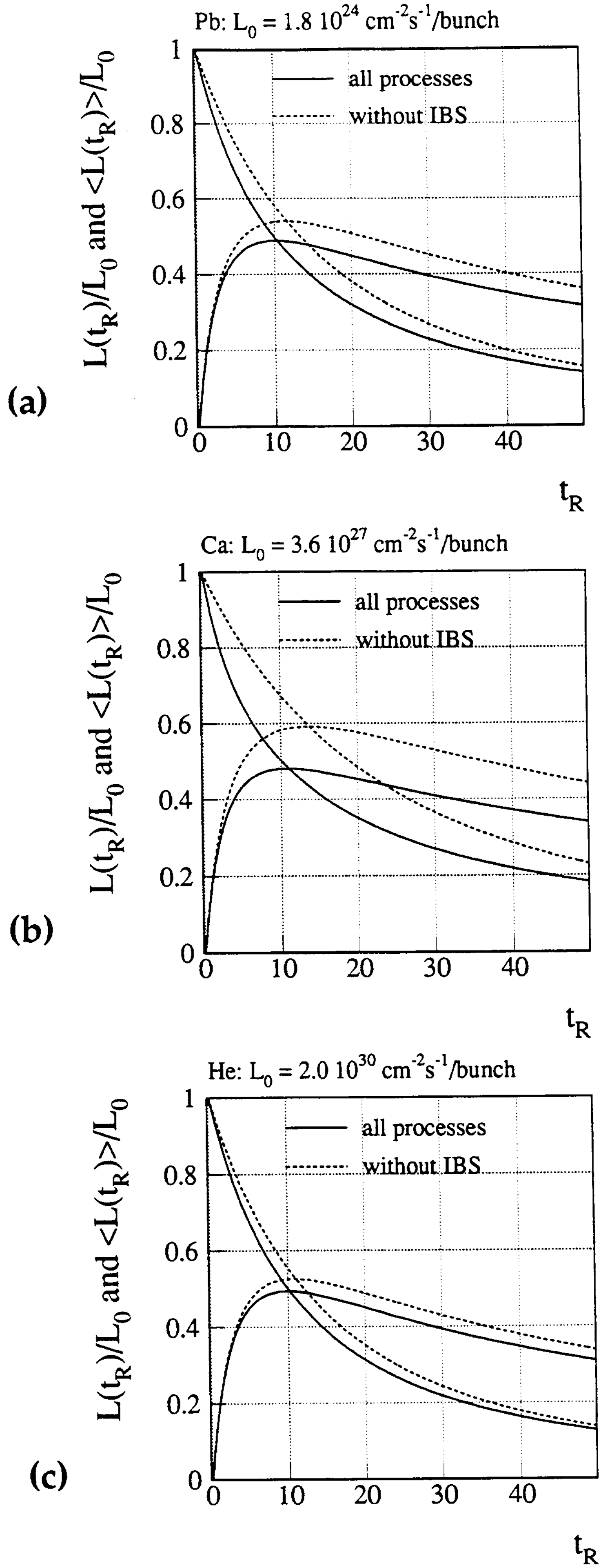

Pb: L_0 = 1.8 10^{24} $cm^{-2}s^{-1}$/bunch
all processes
without IBS
$L(t_R)/L_0$ and $<L(t_R)>/L_0$
t_R
(a)
Ca: L_0 = 3.6 10^{27} $cm^{-2}s^{-1}$/bunch
all processes
without IBS
$L(t_R)/L_0$ and $<L(t_R)>/L_0$
t_R
(b)
He: L_0 = 2.0 10^{30} $cm^{-2}s^{-1}$/bunch
all processes
without IBS
$L(t_R)/L_0$ and $<L(t_R)>/L_0$
t_R
(c)

Fig. 2

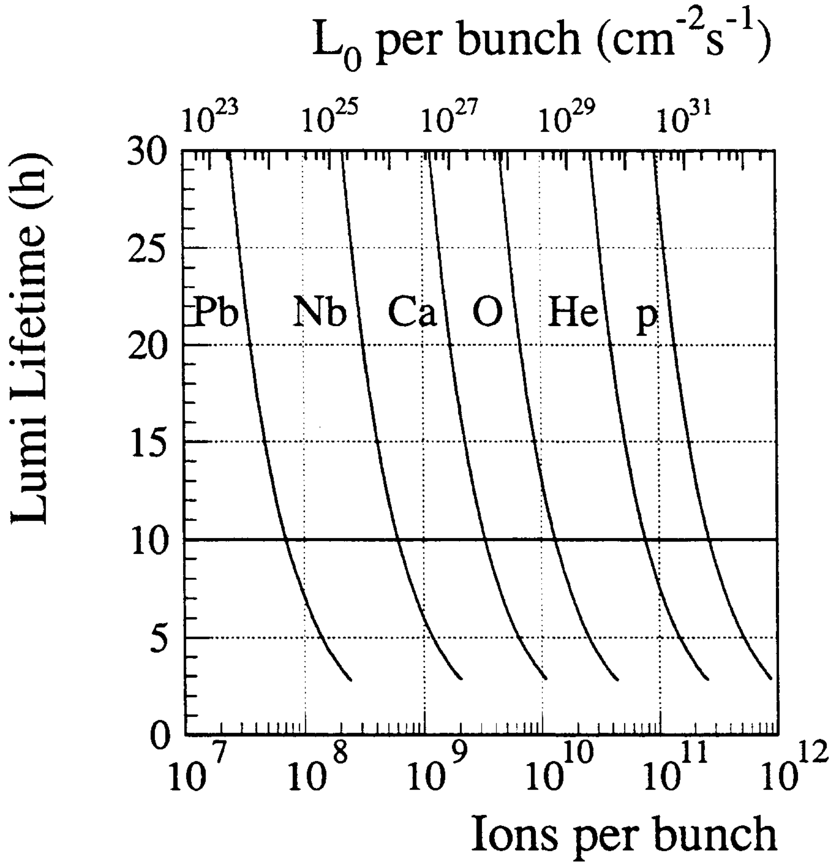

(a) 1 Experiment

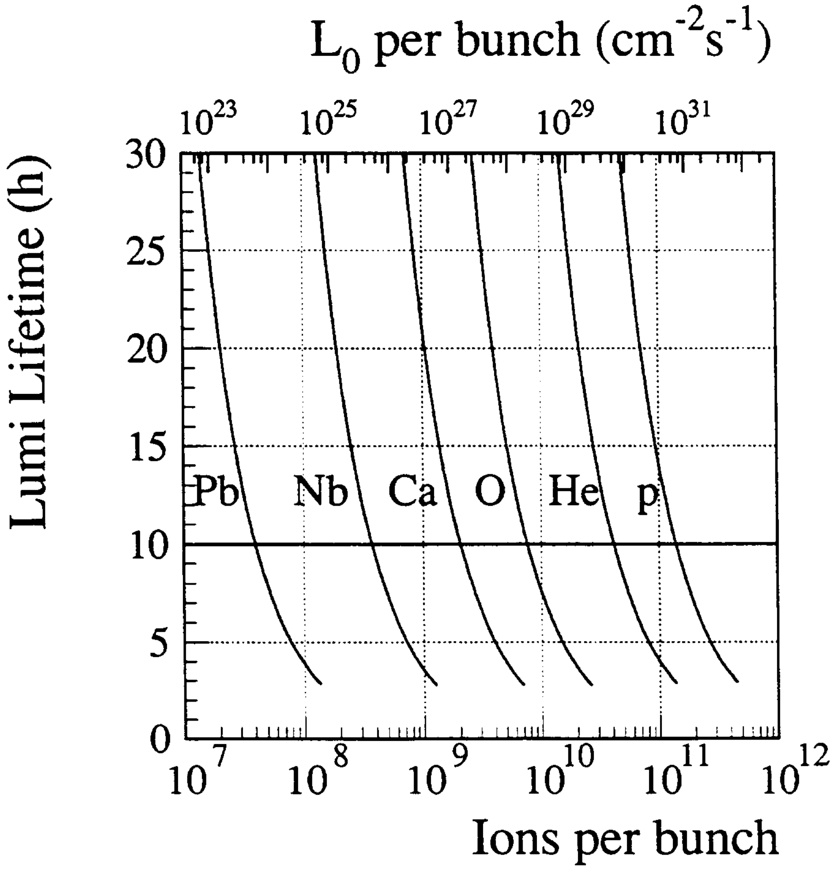

(b) 2 Experiments

Fig. 3

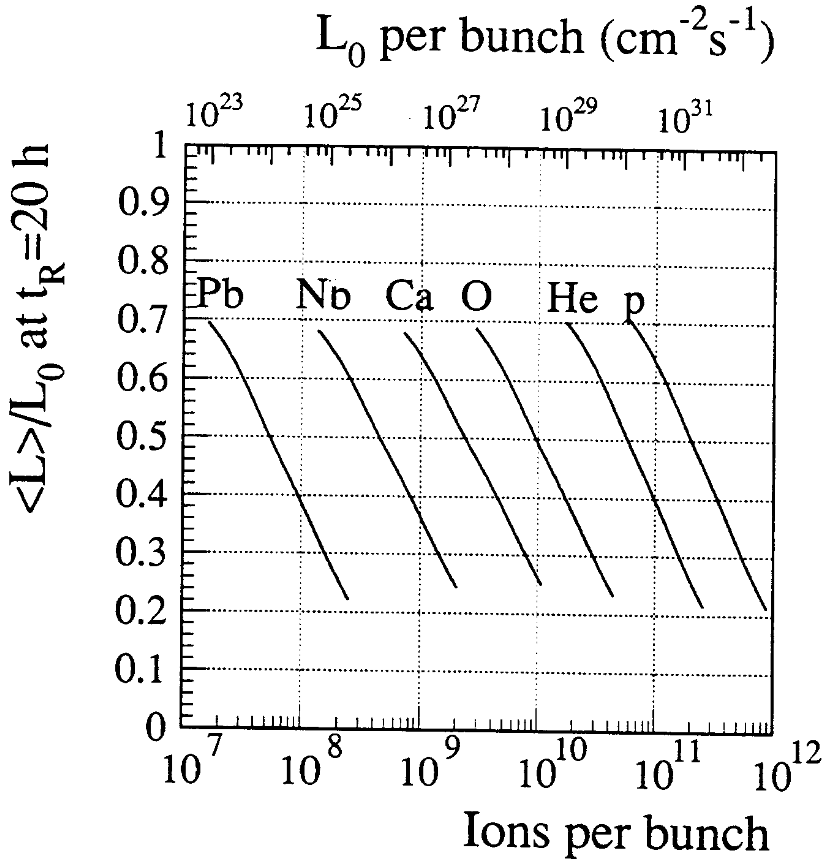

(a) 1 Experiment

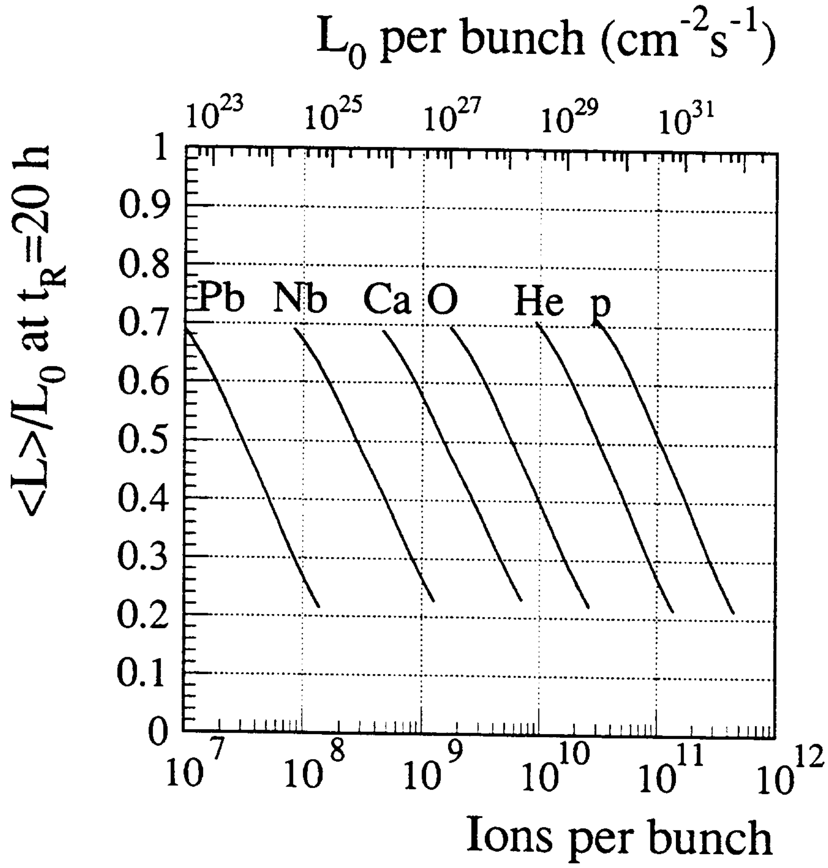

(b) 2 Experiments

Fig. 4

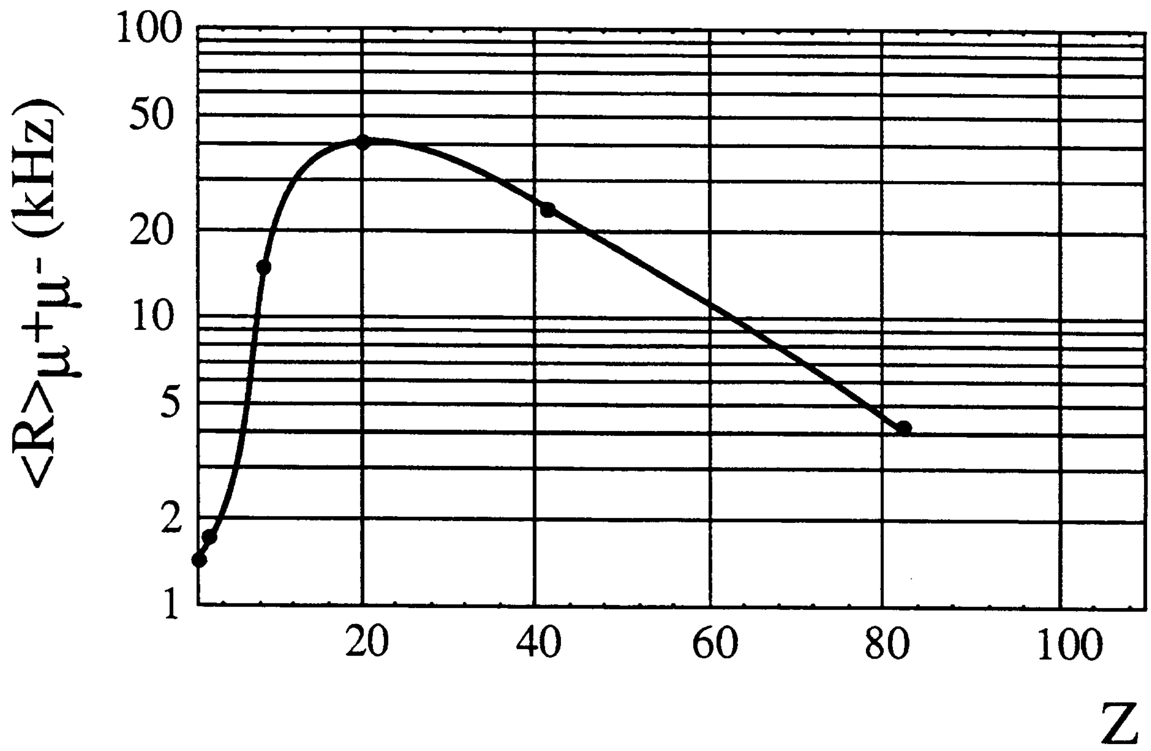

Fig. 5